Effects of the blade shape on the slicing of soft gels

Serge Mora

Effects of the blade shape on the slicing of soft gels

Serge Mora[a]

Laboratoire de Mécanique et Génie Civil, Université de Montpellier and CNRS, Montpellier, France

Abstract Slicing soft gels with a knife is eased by rapidly sliding the blade along its edge. This common observation has been recently explained thanks to a model in which the split of the gel results from a failure occurring at a critical stress and consisting of the transformation of the solid gel into a liquid phase (Phys Rev Lett 125:038002, 2020). Here, the cutting process is shown to be independent of the yield criterion of the gel, and the model investigated further by considering the thickness and the shape of the blade. Features of the slicing process converge toward the zero-thickness limit as the sharpness of the blade increases. The model does predict that a thinner edge facilitates the cleavage. In addition, a symmetric cross section of the blade is found to be more efficient than a bevel.

1 Introduction

Dragging the blade along its edge facilitates the slicing of soft materials: cutting cheese, meat or vegetables is made easier by sliding rapidly the knife rather than just squeezing normally the surface [2,3]. It is also the case for a surgeon precisely cutting into human flesh [4]. This article is focused on the slicing of gels, with which the above examples have strong connections. A gel is a complex system consisting of two phases typically composed of a solid dispersed in a liquid [5,6]. The majority of their mass is that of the liquid, yet they exhibit the properties of a solid, such as a nonzero yield stress [7]. Their physical behaviour results from the formation of percolating networks (made of colloidal particles and/or polymers) and from the interplay between these structures and the fluid [8,9]. This leads to specific properties, making gels used in a broad range of applications [10].

For most solid materials, if the stress remains below a critical value, called later σ_1, the deformation is elastic and the material returns to its original shape after the applied stress is removed. In contrast, a part of the deformation is permanent and non-reversible if this critical stress is passed, corresponding to a plastic behaviour[11].

In gels in which the large majority of the mass comes from the solvent and beyond the critical stress, once a big enough proportion of links forming the gel skeleton is broken, the network disappears and the gel becomes locally a liquid suspension of small particles without the cohesiveness of a solid. This results in viscous liquid-like medium in areas where the stress exceeds the critical stress [12–14]. The critical stress σ_1 is linked with the stress tensor by a general relationship, called yielding criterion, whose expression only depends on the material properties. Because the yielding criterion has to be frame independent, it is a function of the invariants of the stress tensor. Several yielding criteria have been proposed, for different kinds of materials. For isotropic materials, common yield criteria are the Tresca, the von Mises, the Burzyński-Yagn and the Mohr–Coulomb yield criteria [15,16].

A model describing the slicing of soft gels has been recently introduced in [1]. In this model, the blade itself does not contact the network of the gel but slides through the viscous liquid medium resulting from the gel failure occurring at the vicinity of the blade. The cutting force is transmitted from the blade to the solid gel by this thin viscous layer of liquid (see Fig. 1). Whether the deformations of the solid phase are large or small [17,18] does not matter in the theory, the important property being that the gel remains elastic below a critical stress. The goals of this article are to elucidate the role of the yielding criterion on the slicing process and to test the predictions of the model for different geometries of the blade.

The paper is organized as follows. The base equations modelling the slicing and established in [1] are first recalled in Sect. 2, and the choice of the yielding criterion is shown to be definitely unimportant. The effects of the blade thickness are investigated in Sect. 3: the thickness of the liquid layer along the blade is calculated. The main geometrical features of the notch, whose boundary is the solid–liquid interface, are also determined numerically. Steady states in the cutting exist only if the ratio of the normal to the tangential

[a] e-mail: serge.mora@umontpellier.fr (corresponding author)

velocities is lower than a critical value, called here ζ^*. In Sect. 3, ζ^* is computed as a function of the blade thickness. It decreases with the thickness of the blade, meaning that a steady slicing requires a smaller tangential velocity as the blade is thinner. The effect of the angle of a wedge at the cutting edge is investigated in Sect. 4. The model properly predicts that slicing is facilitated by the sharpness of the blade. Then, the case of a bevelled blade is considered. The last section is devoted to a discussion and a conclusion.

2 Base equations for the slicing of a soft gel

In the model, the gels are elastic materials that locally turn into a liquid-like viscous medium if the stress is larger than a critical value, σ_1. This results in a coupling between elasticity and the dynamics of a viscous fluid. In order to bring out the main relevant physical mechanisms, we describe the viscous features of the fluid phase as for a Newtonian liquid, and we do not focus on the detailed rheological behaviour of the fluid phase. Considering other specific constitutive laws would only provide corrections without generality.

In this section, the equations describing this coupling are presented, and the choice of the yielding criterion is discussed.

Following the model introduced in [1], let us consider a blade moving parallel to the edge in the sliding direction at velocity W, this direction being parallel to the surface to be separated. The blade is also moving inward the solid material in the direction perpendicular to the cutting edge at velocity U (Fig. 1).

Let η be the shear viscosity of the liquid phase and let us define the characteristic length ℓ of the system such that the viscous shear stress $\eta W/\ell$ is equal to the yield stress σ_1:

$$\ell = \eta W/\sigma_1. \tag{1}$$

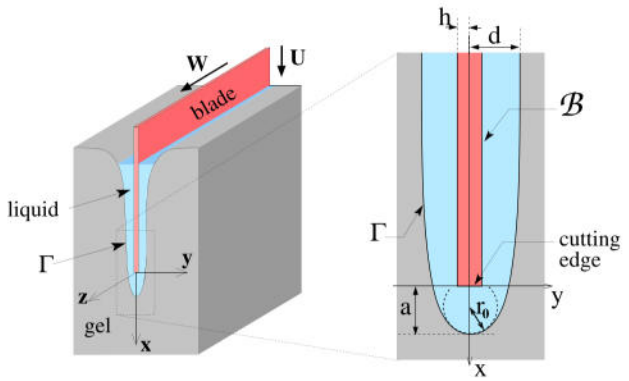

Fig. 1 Sketch of the blade (in red) moving at velocity U in the cutting (normal) direction x and at velocity W in the sliding direction z (parallel to the initial surface of the gel). Here the blade $\mathcal{B}$ is parallelepidic with the thickness $2h$. The boundary of the notch corresponds to the solid–liquid interface, denoted Γ. $2d$ is the lateral extension of the fluid layer behind the cutting edge. a is the distance between the cutting edge and the tip of the notch, and r_0 is the radius of curvature of Γ at the tip of the notch

One can anticipate that ℓ gives the typical thickness of the viscous layer on either side of the blade. Let us estimate orders of magnitude. Consider a hydrogel with a shear yield stress equal to $\sigma_1 = 100$Pa, being cut with the sliding (tangential) velocity $W = 1\text{m s}^{-1}$. The viscosity of the liquid phase is expected to be larger than that of water: we take here $\eta = 1 \times 10^{-2}$Pa s. With these values, the characteristic length defined just above is $\ell = 100\mu$m, which is a relevant length scale in the context of continuum mechanics.

The order of magnitude of the rate of migration of the solvent into the solid phase due to the stress generated by the cutting is important in order to determine whether the solid phase can be approximated as incompressible. The shear modulus of the gel is expected to be of order kT/ξ^3 where ξ is the mesh size of the gel [19]. The yield stress σ_1 being usually comparable to the shear modulus, one gets, again with $\sigma_1 = 100$Pa, $\xi \sim 30$nm. Considering a Poiseuille flow through the porous medium of mesh size ξ resulting from a pressure gradient ∇p, the characteristic permeation velocity inside the gel is $v_{liq} \sim \frac{\xi^2 \nabla p}{\eta_{gel}}$. With $\eta_{gel} = 1$mPa s, $\xi = 30$nm and $\nabla p \sim \frac{\sigma_1}{\ell} \sim 1 \times 10^6$Pa m^{-1}, one obtains $v_{liq} \sim 1 \times 10^{-6}$m s^{-1}, a velocity far smaller than U and W. Hence, the solid phase will be considered in this paper as incompressible.

In the following, x is the direction normal to the initial gel surface, y is the direction perpendicular to the plane of the knife, and z is the direction of the sliding. y and z are therefore parallel to the initial free surface of the material. The width of the blade (along z) is assumed to be far larger than the other length scales, so that the system can be considered as invariant along z.

The blade is supposed to have advanced in the solid gel for a sufficiently long time and to continue to separate it at constant velocities, making a self-reproducing notch in the gel around the cutting edge and leading to a steady state. Within these assumptions, the notch boundary is stationary in the frame moving with the knife and the solid gel has a homogeneous velocity. This velocity is $-W$ in the sliding direction and $-U$ toward the blade. In the frame moving with the knife, let u, v, w be the velocity component in the viscous liquid surrounding the blade, along x, y and z respectively. The system being invariant along z, the incompressibility condition of the liquid is:

$$u_{,x} + v_{,y} = 0, \tag{2}$$

where $u_{,x} = \frac{\partial u}{\partial x}$, etc. The Reynolds number in the liquid is assumed to be low enough to make valid the linear Stokes equation:

$$\eta(u_{,xx} + u_{,yy}) = p_{,x}, \tag{3}$$
$$\eta(v_{,xx} + v_{,yy}) = p_{,y}, \tag{4}$$
$$w_{,xx} + w_{,yy} = 0, \tag{5}$$

with p the pressure.

In the frame moving with the knife, the fluid velocity is zero on the surface $\mathcal{B}$ of the blade (see Fig. 1), hence $(u, v, w) = (0, 0, 0)$ on $\mathcal{B}$. Let Γ be the boundary of the cross section of the notch in the plane (x, y), i.e. the projection of the solid–liquid interface onto (x, y). The continuity equation imposes that the flux of matter on the gel side of Γ is equal to the flux of liquid on the other side. Mass densities are almost the same on both sides of Γ. Hence, continuity of the flux of matter implies the continuity of velocity through Γ. Since the components of the velocity on the solid side are $(-U, 0, -W)$ in the frame moving with the knife, the velocity in the liquid along Γ has to fulfil:

$$u|_\Gamma = -U \tag{6}$$
$$v|_\Gamma = 0 \tag{7}$$
$$w|_\Gamma = -W \tag{8}$$

The Cauchy stress tensor in the liquid phase is $\underline{\underline{\sigma}} = \underline{\underline{\tilde{\sigma}}} + p\mathbb{I}$ with $\mathbb{I}$ the identity tensor and $\underline{\underline{\tilde{\sigma}}}$ the deviatoric stress given by the standard formulae for viscous fluids [20],

$$\underline{\underline{\tilde{\sigma}}} = \eta \begin{pmatrix} 2u_{,x} & u_{,y} + v_{,x} & w_{,x} \\ u_{,y} + v_{,x} & -2u_{,x} & w_{,y} \\ w_{,x} & w_{,y} & 0 \end{pmatrix}. \tag{9}$$

The interfacial tension between the two phases is negligible because the gel is mainly composed of solvent, the same as the liquid phase [21,22]. In addition, we consider boundary conditions such that the gel is not initially stressed, so that the stress in the gel at the interface Γ is the viscous stress applied by the liquid on the gel, $\underline{\underline{\sigma}}$. The characteristic polynomial of $\underline{\underline{\tilde{\sigma}}}$ is as a function of the variable σ:

$$\begin{aligned} &-\sigma^3 + \eta^2 \left(w_{,y}^2 + w_{,x}^2 + 4u_{,x}^2 + (u_{,y} + v_{,x})^2\right)\sigma \\ &+\eta^3 \left(-2u_{,x}w_{,y}^2 + 2(u_{,y} + v_{,x})w_{,x}w_{,y} + 2u_{,x}w_{,x}^2\right). \end{aligned} \tag{10}$$

From Eqs. 6-8, the derivatives of u, v and w along Γ, defined here as $x = \Gamma(y)$, are equal to zero. Hence, at the gel–fluid interface, $u_{,x}\Gamma_{,y} + u_{,y} = 0$, $v_{,x}\Gamma_{,y} + v_{,y} = 0$ and $w_{,x}\Gamma_{,y} + w_{,y} = 0$. As a consequence, the characteristic polynomial of $\underline{\underline{\tilde{\sigma}}}$ (Eq. 10) simplifies with Eq. 2, for $(x, y) = (\Gamma(y), y)$, in:

$$-\sigma^3 + \eta^2 \left(w_{,y}^2 + w_{,x}^2 + 4u_{,x}^2 + (u_{,y} + v_{,x})^2\right)\sigma, \tag{11}$$

and the principal stresses, defined as the eigenvalues of $\underline{\underline{\tilde{\sigma}}}$, are 0 and $\pm\Sigma$ with

$$\Sigma = \eta\sqrt{w_{,y}^2 + w_{,x}^2 + 4u_{,x}^2 + (u_{,y} + v_{,x})^2}. \tag{12}$$

The solid–fluid interface is then subjected to a pure shear stress. For a isotropic material, the critical stress σ_1 for the solid–liquid transformation has to be independent on the choice of coordinates. Hence, for an incompressible solid, it has to be a function of the eigenvalues of $\underline{\underline{\tilde{\sigma}}}$, here a function of Σ:

$$\sigma_1 = f(\Sigma). \tag{13}$$

Taking for σ_1 the shear yield stress of the gel [23] in the region around the tip of the notch where liquefaction is happening, the equation of the curve Γ is found by imposing the condition

$$\Sigma = \sigma_1 \tag{14}$$

on Γ, whatever the yielding criterion specific to the gel. The details of the yield criterion are here irrelevant. The only assumptions that have to be made about the mechanical behaviour of the gel are (i) the solid phase is isotropic and incompressible, and (ii) it behaves as a Newtonian liquid beyond the yielding point.

In the following, ℓ (defined in Eq. 1) is taken as unit length, W as unit speed and σ_1 as unit stress. In addition, the ratio of the normal to the tangential velocity, U/W, is called ζ.

3 Blades with a finite thickness

In [1], the blade was assumed to be sharp enough to be approximated as a half plane of zero thickness. We consider here straight blades (i.e. blades with parallel edges) of finite thickness $2h$, and we compute the shape of the solid–liquid interface (Γ) as well as the critical tangential velocity. We show that they converge towards the zero-thickness solution as the finite thickness of the blade tends to zero.

Let us first compute the characteristic thickness of the liquid layer in the liquefaction region *behind* the cutting edge of the blade (see Fig. 1). This thickness is defined as $d - h$, where $2d$ is the total extension of the cross section of the notch behind the cutting edge, as indicated in Fig. 1. In this region, derivatives along x-direction in Eq. 12 are negligible and Eq. 12 simplifies:

$$\Sigma = \eta\sqrt{w_{,y}^2 + u_{,y}^2}. \tag{15}$$

According to the incompressibility condition (Eq. 2), the average value of u along y is $< u >= -\frac{d}{d-h}U$. From Eq. 4, $u(y)$ is parabolic and from the boundary conditions at $y = 0$ and $y = d$, the velocity profile for $-x \gg \ell$ and $-x \gg (d - h)$ is:

$$u(y) = 3U\frac{d+h}{d-h}\left(\frac{y-h}{d-h}\right)^2 - 2U\frac{2d+h}{d-h}\left(\frac{y-h}{d-h}\right). \tag{16}$$

This is a simple combination of Couette and Poiseuille flows [24], the pressure gradient along the x-direction being constant (see Fig. 2). In addition, $w(y)$ is linear

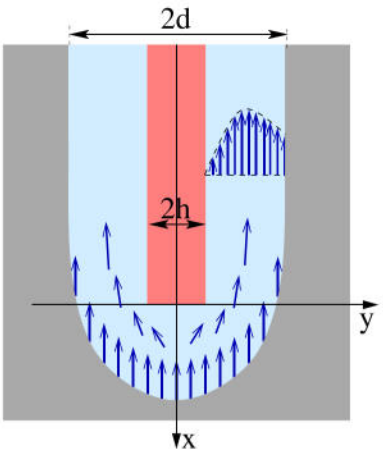

Fig. 2 Sketch of a cross section of the notch near the cutting edge, in the plane (x, y). The blade is drawn in red, the solid gel in grey, the liquid in light blue, and the velocity field in plane (x, y) is represented in heavy blue

(Couette flow without pressure gradient):

$$w(y) = -W\frac{y-h}{d-h}. \tag{17}$$

One concludes from Eqs. 15-17 that for $-x \gg -\ell$ and $-x \gg (d-h)$,

$$\Sigma = \frac{\eta}{d-h}\sqrt{\left(\frac{2d+4h}{d-h}\right)^2 U^2 + W^2}, \tag{18}$$

and from Eq. 14, the thickness $d-h$ of the liquid layer along the blade is found by solving the equation:

$$\frac{1}{\ell} = \frac{1}{d-h}\sqrt{\left(\frac{2d+4h}{d-h}\right)^2 \zeta^2 + 1}. \tag{19}$$

$(d-h)/\ell$ is plotted as a function of ζ for two values of h/ℓ in Fig. 5c, $h = 0.3\ell$ and $h = 0.01\ell$. The thickness of the liquid layer behind the cutting edge increases as the thickness of the blade increases. This behaviour can be explained by considering the velocity components in plane (x, y) and the incompressibility condition (Eq. 2). The liquid produced by the part of Γ facing the cutting edge (parallel to y) is evacuated on either side of the blade. Consequently, an increase in the blade thickness generates an increase in the flow rate along the blade. The thickness of the liquid layer has therefore to be larger in order to maintain the viscous shear stress Σ equal to σ_1 (see Fig. 2).

Details of the shape of the notch are computed following the method used in [1]. Eqs. 2-5 together with Eq. 14 are solved using the finite-element method, implemented in the open-source finite-element library FEniCS [25]. The origin of coordinates (x, y) is chosen such that the middle of the cutting edge is at $(x, y) = (0, 0)$ (Fig. 2). For convenience, the curve Γ

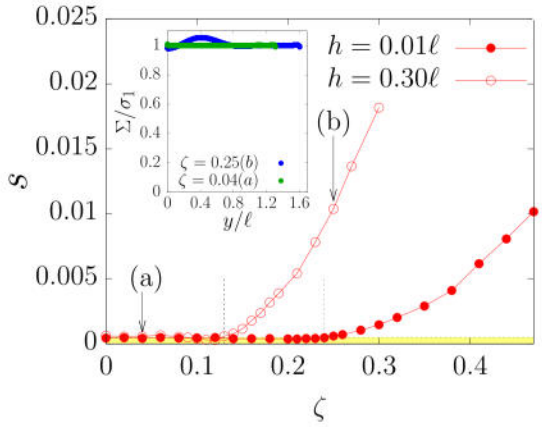

Fig. 3 Standard deviation s (as defined in Eq. 21) for the best fit of Eq. 20, as a function of ζ, for straight blades of half-thickness $h = 0.01\ell$ and $h = 0.3\ell$. Inset : example of reduced stress Σ/σ_1 calculated along the solid–liquid interface for $\Gamma(y)$ resulting from the best fit, in the case of a blade of half-thickness $h = 0.3\ell$, and for $\zeta = 0.04$ and $\zeta = 0.25$. The condition $\Sigma = \sigma_1$ (Eq. 14) is well approached for $\zeta = 0.04$, while discrepancies are observable for $\zeta = 0.25$, indicating that condition $\Sigma = \sigma_1$ cannot be fulfilled in this case. This is because $\zeta^* = 0.125 \pm 0.05 > 0.25$

is defined as $x = \pm\Gamma(y)$. For $-d \le y \le d$, $\Gamma(y)$ is expanded as

$$\Gamma(y) = a + \sum_{k=1}^{n-1} \alpha_{2k}(y/d)^{2k} + \alpha_n \sum_{k=n}^{m} (y/d)^{2k} \text{ for } -d \le y \le d. \tag{20}$$

a is the distance between the cutting edge and the tip of the notch (see Fig. 1). The first two terms of the right-hand side are a truncated Taylor series. In the second term, n has to be big enough in order to describe in a good approximation the interface far enough from the tip of the notch. The third term is here to ensures a smoother profile of the notch as $\gamma(y)$ tends to d. In the computations, x is in the range $[x_{min}, a]$ with $x_{min} < \Gamma(d)$. y is set to $\pm d$ for x in $[x_{min}, \Gamma(d)]$, with $|x_{min}|/\ell = 9$. In the following, $n = 8$ and $m = 20$, and we have checked that neither an increase in n, in m nor in $|x_{min}|/\ell$ induce significant changes on the results presented below. Velocities u, v, w are discretized using quadratic continuous Lagrange finite element functions and the pressure by linear Lagrange finite element functions. Coefficients α_{2k} together with a are fitted using a Gradient descent procedure in order to fulfil Eq. 14.

Let us define the standard deviation s of the fit as

$$s^2 = \frac{1}{2 \times 0.95d}\int_{-0.95d}^{0.95d} \frac{(\Sigma(y) - \sigma_1)^2}{\sigma_1^2} \mathrm{d}y, \tag{21}$$

The interval $[-0.95d, 0.95d]$ in the integral of Eq. 21 excludes the contribution of the parallel flanks of the notch, far from the tip. s quantifies the accuracy of the best trial for Γ, using Eq. 20. In Fig. 3, s is plotted as a function of ζ for two different thicknesses, $h = 0.01\ell$ (thin blade) and $h = 0.3\ell$ (thicker blade). It starts to

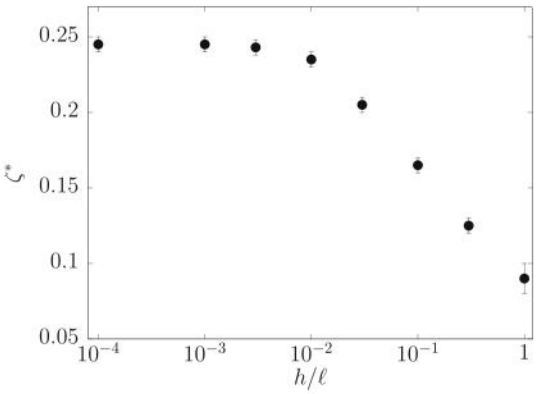

Fig. 4 Critical normal to tangential velocity ratio, ζ^*, as a function of half of the relative thickness of the blade, h/ℓ. For each value of h/ℓ, ζ^* has been determined from a series of fits carried out for different values of ζ, as shown in Fig. 3 for $h = 0.01\ell$ and $h = 0.3\ell$

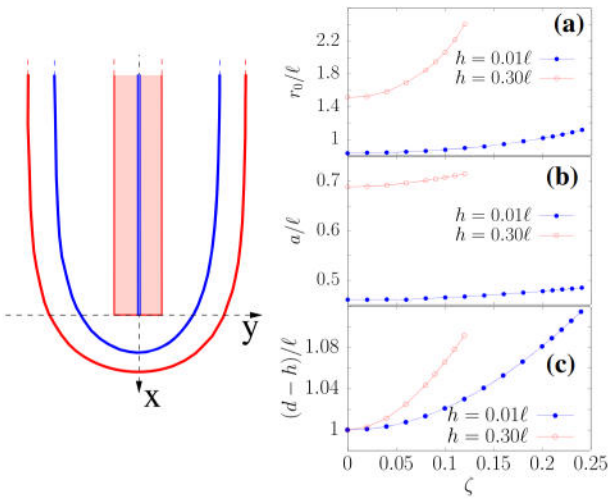

Fig. 5 Left panel: cross section of the notches for $\zeta = 0.1$ and $h = 0.01\ell$ (blue) and $h = 0.3\ell$ (red), computed from the best fit. The blades are represented by the filled rectangles (blue and red), and the boundaries of the liquid–solid interfaces are represented by the curved lines. Right panels: reduced radius at the tip of the notch obtained from the best fits (**a**), reduced distance between the tip of the notch and the cutting edge obtained from the best fits (**b**) and reduced thickness of the liquid layer along the blade obtained by the best fit or from Eq. 19 (indistinguishable) (**c**), as functions of ζ for $h = 0.01\ell$ (blue) and $h = 0.3\ell$ (red)

grow up beyond a certain value of ζ, called later ζ^*: for $\zeta < \zeta^*$, the profile Γ deduced from the fit procedure well captures the condition Eq. 14, in contrast with $\zeta > \zeta^*$ where no profile fulfilling Eq. 14 is found (see inset of Fig. 3). ζ^* depends on the relative thickness of the blade. For $h/\ell \ll 1$, ζ^* tends to 0.245 ± 0.005, in agreement with the case of a blade modelled as a half plane [1]: the solution of the slicing with blades of finite thickness converges well toward the solution obtained with an idealized blade of zero thickness. ζ^* is found to decrease as h/ℓ increases (Fig. 4). Hence, if ℓ (i.e. the ratio $\sigma_1/(\eta W)$) is fixed, the maximum cutting (normal) velocity for a steady state decreases as the blade thickness increases : steady slicing requires a lower tangential velocity as the blade is thinner. Indeed, for a given blade thickness $2h$, an increase in the tangential velocity (W) leads to a higher maximum cutting velocity $U_{max} = \zeta^* W$ because W and also ζ^* are larger (the characteristic length $\ell = \frac{\eta W}{\sigma_1}$ growths upon an increase in W, hence ζ^* also growths, as shown in Fig. 4): A higher tangential velocity definitely allows quicker dicing.

The values of a/ℓ and the reduced radius of curvature $r_0/\ell = h^2/(2\alpha_2^2)$ are plotted as a function of ζ (for $\zeta < \zeta^*$) in Fig. 5b. a/ℓ increases with ζ. This behaviour can be explained as follows: for a fixed value of the tangential velocity W, increasing $\zeta = U/W$ means increasing U. Hence, to maintain the viscous shear stress equal to σ_1 at the tip of the notch while ζ rises, the distance a, or equivalently a/ℓ, has to be augmented.

Beyond the variation of a/ℓ with ζ, a/ℓ increases as h/ℓ is larger. This is a consequence of the incompressibility of the liquid: the fluid produced by the tip of the notch is evacuated along the blade, the thickness of the blade making the flow convergent (see Fig. 2). Hence, the fluid velocity increases (still considering the frame moving with the blade), requiring a larger distance a to maintain the viscous shear stress equal to σ_1 at the tip of the notch.

As previously reported, the radius of curvature at the tip of the notch grows with ζ (Fig. 5a). Moreover, it is bigger as the thickness of the blade is larger due to the geometrical constraints imposed by the thickness of the blade.

Note that r_0/ℓ, a/ℓ and $(d-h)/\ell$ also converge toward the values previously found [1] in the limit of the blade modelled by a half plane.

A thinner blade is known, from observations made in everyday life, to facilitate the cutting. The common explanation is that for a given applied force, a thinner edge generates higher stresses in the cutting zone, and therefore makes it easier to reach the critical stress at which the material fails. Thanks to the model investigated here, this explanation can be refined: For a given tangential velocity, the shear stress produced by this tangential velocity at the tip of the notch is higher as the blade is thinner since a decreases as the blade is thinner (as previously seen, Fig. 5b).

4 Wedge at the cutting edge of the blade

Reducing the blade thickness (as in Sect. 3) in order to facilitate the cutting necessarily makes it more breakable. An other route is to consider blades with a sharp wedge at the cutting edge. In this section, we investigate the effect of the terminal angle of the wedge (see Fig. 6).

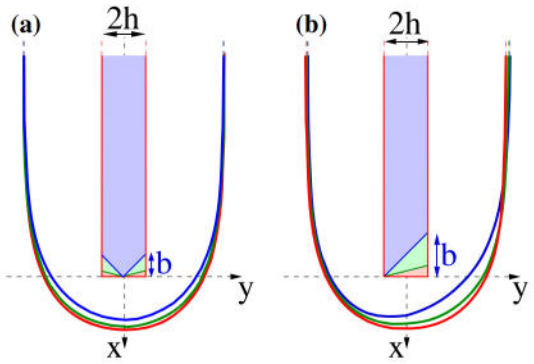

Fig. 6 Examples of cross sections (Γ) of the solid–liquid interface for blades of half-thickness $h = 0.3\ell$, with a tangential to normal velocity ratio $\zeta = 0.1$, and various depths b of the wedge or the bevel. **a** Symmetric blades with $b = 0$, $b = 0.25\ell$ and $b = \ell$. **b** Asymmetric blades with $b = 0$ (red), $b = 0.5\ell$ (green) and $b = 2\ell$ (blue). Note that these values of b have been chosen so that the angle formed by the inclined face of the blades with axis y are the same from (**a**) to (**b**)

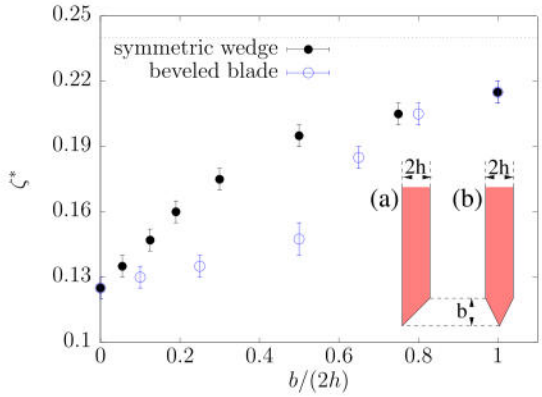

Fig. 7 Critical normal to tangential velocity ratio, ζ^*, as a function of $b/(2h)$, for blades of thickness $2h = 0.6\ell$, with a symmetric wedge at the cutting edge (black disks) and with a bevelled (blue circles). Dashed line indicates the value of ζ^* found for blades modelled as a half plane. Inset: reminder of the shape of the cross section of a blade with a terminal symmetric wedge (**a**), and a bevelled blade (**b**)

We focus on two geometries: symmetric wedges (Fig. 6a) and bevelled blades (Fig. 6b). Let b be the depth of the wedge or the bevel, and $2h$ be the terminal thickness of the blade (above the wedge or the bevel). In what follows, the thickness of the blade is fixed to $2h = 0.6\ell$. Fits have been made following the procedure explained in Sect. 3, with the new geometries of the blade. Γ is again defined by Eq. 20 in the symmetric case. For bevelled blades, the reflection symmetry with respect to y is lost and we take for Γ :

$$\Gamma(y) = a + \sum_{k=1}^{n-1} \alpha_k \left(\frac{y-y_0}{d}\right)^k + \alpha_n \sum_{k=n}^{m} \left(\frac{y-y_0}{d}\right)^{2k} \quad \text{for} \quad -d \le y \le d. \tag{22}$$

A transverse shift of Γ is made possible thanks to y_0. Some cross sections are shown in Fig. 6 for symmetric blades and for bevelled blades, for the velocity ratio $\zeta = 0.1$. As expected, the cross section is not symmetrical anymore with bevelled blades: The fluid layer behind the cutting edge of the blades is thinner on the side of the tip (on the left of the blades in Fig. 6b) than on the other side. In both cases (symmetric or bevelled), the distance between the tip of the blades and that of the notch decreases as the angle is sharper. This is because the in-plane fluid velocity is smaller as the wedge is sharper since the incompressible fluid has a larger area to flow as the angle of the wedge is smaller. Hence, a shorter distance a/ℓ is required to a produce viscous stress equal to σ_1.

The critical ratio ζ^* of the normal to the tangential velocity is plotted as a function of $b/(2h)$ in Fig 7. Steady cutting with a sharper blade necessitates smaller tangential velocity.

This is reminiscent with the conclusion of Sect. 3 since the "average thickness" of the blade close to the cutting edge is thinner as the blade is sharper. Interestingly, ζ^* is found to be smaller in the case of bevelled blades for certain values of $b/(2h)$ (Fig. 7), showing that the maximum cutting velocity (U) is larger, for a given W, with a symmetric wedge.

5 Discussion

The slicing of gels has been described by a model in which the solid is transformed into a Newtonian liquid beyond a prescribed value of the shear stress. The blade is surrounded by a viscous liquid layer, and the applied stress is transmitted to the solid by this viscous layer. The validity of the model requires that the characteristic length ℓ be macroscopic, hence that the critical stress be small enough. For instance, for a tangential velocity equal to $W = 1\text{m s}^{-1}$ and a liquid viscosity equal to $\eta = 10\text{mPa s}$, σ_1 has to be smaller than 1×10^4 Pa to ensure that ℓ is larger than 1μm.

A steady regime in the slicing necessitates a small enough ratio of the cutting (normal) velocity to the sliding (tangential) velocity: U/W has to be smaller than ζ^*, where ζ^* depends on the blade thickness and on the shape of the cutting edge of the blade. The maximum cutting velocity is therefore directly related to the sliding velocity. A thinner blade is more suitable for slicing rapidly and in addition the cutting is facilitated by the sharpness of the blade, as it allows larger cutting velocity for a given sliding velocity.

The choice of the yielding criterion has no effect on the slicing because the viscous stress exerted by the liquid on the solid at the interface is a pure shear stress. It can therefore be accounted for by a single scalar (σ_1). This reinforces the generality of the predictions

arising from the model, insofar as all these results are valid whatever the choice of the criterion. This should not obscure that the stress induced transformation of the solid into a liquid is a complex phenomenon. Some assumptions have led to simplifications in the model.

First, describing the material properties in the process zone as a Newtonian fluid is a simplifying hypothesis. The rheological features of this zone may be more complex. It would be interesting to consider constitutive equations accounting for specific rheological properties, such as those of Bingham fluids [26,27]. Reducing them to a Newtonian fluid must be viewed as a first approximation in order to bring out the important physical mechanisms in the slicing process. The goal is to take into account the viscous effects of the fluid in the model, in a simple although realistic and relevant form.

A finite width of the transition zone from solid to liquid has not been considered here, by assuming this width is far smaller than ℓ. In addition, the transformation of the solid to liquid for stress beyond σ_1 is not instantaneous. We have considered in the model that the timescale ℓ/U related to the penetration of the blade into the gel is much larger than the characteristic time involved in the solid–liquid transformation [28]. Introducing more detailed constitutive laws taking into account internal characteristic times of the material would be useful, for instance to deal with thixotropic fluids [29].

In this paper, we have focused on steady states. A better understanding of the early stages of the slicing by considering transient regimes would be useful, giving hints for elucidating the physics of slicing in the cases no steady state exists, i.e. when the normal velocity is too fast compared to the tangential one. Hence, completing the model by taking into account time dependence is an important task that has now to be addressed.

Comparisons of the theoretical predictions with experiments would be welcome, and experiments could reveal what happen in the cases no steady state exists. Unfortunately, experimental data for a quantitative or even semi-quantitative comparison with the theory are currently lacking. Cutting with sliding soft materials has been explored only for relatively slow tangential (and normal) velocities [3,30] so that the characteristic length (ℓ) is too small to be relevant at the continuous scale. In addition, these experimental data mainly concern situations for which the ratio of tangential to normal velocities is larger than one [3,30], and data with a ratio less than one are far too spare to draw any tendency.

Acknowledgements The author wishes to thank Yves for Pomeau very inspiring discussions. The author thanks also one anonymous reviewer for her/his relevant suggestions.

References

1. S. Mora, Y. Pomeau, Cutting and slicing weak solids. Phys. Rev. Lett. **125**, 038002 (2020)
2. T. Atkins, Optimum blade configurations for the cutting of soft solids. Eng. Fract. Mech. **73**, 2523–2531 (2006)
3. E. Reyssat, T. Tallinen, M. Le Merrer, L. Mahadevan, Slicing softly with shear. Phys. Rev. Lett **109**, 244301 (2012)
4. L.P. Sturm, J.A. Windsor, P.H. Cosman, P. Cregan, P.J. Hewett, G.J. Maddern, A systematic review of skills transfer after surgical simulation training. Ann. Surg. **248**, 166–179 (2008)
5. I. Sakai, *Physics of Polymer Gels* (Wiley-VCH Verlag, Weinheim, 2020)
6. A. Fernandez-Nieves, A.M. Puertas, *Fluids, Colloids and Soft Materials: An Introduction to Soft Matter Physics* (Wiley, Hoboken, 2016)
7. D. Bonn, M.M. Denn, L. Berthier, T. Divoux, S. Manneville, Yield stress materials in soft condensed matter. Rev. Mod. Phys. **89**, 035005 (2017)
8. C.W. Macosko, *Rheology: Principles, Measurements, and Applications* (Wiley-Blackwell, New York, 1994)
9. K.A. Whitaker, Z. Varga, L.C. Hsiao, M.J. Solomon, J.W. Swan, E.M. Furst, Colloidal gel elasticity arises from the packing of locally glassy clusters. Nat. Commun. **10**, 2237 (2019)
10. U. Demirci, A. Khademhonneini, *Gels Handbook: Fundamentals, Properties* (World Scientific Publishing Company, Applications, 2016)
11. F.P. Beer, E.R. Johnston, J.T. Dewolf, *Mechanics of Materials* (McGraw-Hill, New-York, 2001)
12. M. Cloitre, M. Borrega, F. Monti, L. Leibler, Glassy dynamics and flow properties of soft colloidal pastes. Phys. Rev. Lett. **90**, 068303 (2003)
13. P. Coussot, H. Tabuteau, X. Chateau, L. Tocquer, G. Ovarlez, Aging and solid or liquid behavior in pastes. J. Rheol. **50**, 975 (2006)
14. T. Divoux, C. Barentin, S. Manneville, From stress-induced fluidization processes to herschel-bulkley behaviour in simple yield stress fluids. Soft Matter **7**, 8409 (2011)
15. R. von Mises. Mechanik der festen korper im plastisch-deformablen (1913)
16. R.M. Christensen, *The Theory of Materials Failure* (Oxford University Press, Oxford, 2016)
17. R. Long, C.-Y. Hui, Crack tip fields in soft elastic solids subjected to large quasi-static deformation - a review. Extreme Mech. Lett. **4**, 131–155 (2015)
18. H. Tabuteau, S. Mora, M. Ciccotti, C.-Y. Hui, C. Ligoure, Propagation of a brittle fracture in a viscoelastic fluid. Soft Matter **7**, 9474–9483 (2011)
19. P.G. de Gennes, *Scaling Concepts in Polymer Physics* (Cornell University Press, Ithaca, 1979)
20. L.D. Landau, E.M. Lifshitz, *Fluid Mechanics* (Pergamon Press, Oxford, 1984)
21. S. Mora, C. Maurini, T. Phou, J.M. Fromental, B. Audoly, Y. Pomeau, Solid drops: large capillary deformations of immersed elastic rods. Phys. Rev. Lett. **113**, 178301 (2014)
22. S. Mora, Y. Pomeau, Softening of edges of solids by surface tension. J. Phys. Condens. Matter **27**, 194112 (2015)
23. R. Buscall, P.D.A. Mills, G.E. Yates, Viscoelastic properties of strongly flocculated polystyrene latex dispersions. Colloids Surf. **18**, 341–358 (1986)

24. G.K. Batchelor, *An Introduction to Fluid Dynamics* (Cambridge University Press, Cambridge, 2000)
25. A. Logg, K.A. Mardal, G. Wells, *Automated Solution of Differential Equations by the Finite Element Method* (Springer, Berlin, 2012)
26. G.R. Burgos, A.N. Alexandrou, On the determination of yield surfaces in herschel-bulkley fluids. J. Rheol. **43**, 463 (1999)
27. N.J. Balmforth, I.A. Frigaard, G. Ovarlez, Yielding to stress: recent developments in viscoplastic fluid mechanics. Annu. Rev. Fluid Mech. **46**, 121 (2014)
28. S. Varchanis, S.J. Haward, C.C. Hopkins, A. Syrakos, A.Q. Shen, Y. Dimakopoulos, J. Tsamopoulos, Transition between solid and liquid state of yield-stress fluids under purely extensional deformations. PNAS **117**, 12611–12617 (2020)
29. M. Dinkgreve, M. Fazilati, M.M. Denn, D. Bonn, Carbopol: From a simple to a thixotropic yield stress fluid. J. Rheol. **62**, 773–780 (2018)
30. A.G. Atkins, X. Xu, G. Jeronimidis, Cutting, by 'pressing and slicing', of thin floppy slices of materials illustrated by experiments on cheddar cheese and salami. J. Mater. Sci. **39**, 2761–2766 (2004)